biomechanical simulation,
finite element models,
MRI and CT Data

Frithjof KRUGGEL[*], Marc TITTGEMEYER[*], Gert WOLLNY[*]

CLINICAL APPLICATIONS OF BIOMECHANICAL SIMULATION

The planning of therapeutical interventions and the understanding of pathological processes may be improved by providing tools for biomechanical simulation. This article focuses on computational services providing numerical simulations for analysis, prediction and virtual prototyping to the medical sector ("bio-numerics"). Two example problems are discussed: (1) The simulation of distraction osteogenesis using Finite Element Models (FEM): Simulations use highly resolved meshes in order to represent the complex midface structures with sufficient detail. Meshes with 1 mm resolutions typically have 1+ million nodes, so forward models must be computed on high performance computing (HPC) platforms. Pre-operative planning involves "playing" with different what-if scenarios so fast response times are highly desirable in order to provide tools that are accepted in a clinical environment. (2) Intra-operative planning in neurosurgery using inverse biomechanical models: Surgically induced deformations invalidate pre-operatively acquired information about functionally relevant areas. This problem is addressed by non-linear registration of pre-operative functional Magnetic Resonance Imaging (MRI) data to intra-operative MRI data.

1. INTRODUCTION

The central objective of numerical simulation for bio-medical problems is the improvement of clinical and medical practices. The EU-funded project SimBio [6] aims at constructing a generic environment, running on parallel and distributed computing systems, capable of handling a range of important problems relevant to the target community of clinical and medical service providers. The environment combines sophisticated medical imaging, high-level image processing, finite element techniques, and parallel computing technologies. A key feature is the input of *individual* medical scan data to the modelling and simulation process. The environment consists of the following components: a discrete representation of the physical problem as a finite element mesh; a numerical solution system; a framework for inverse problem and design optimisation; an advanced, problem-targeted visualisation system. We focus here on bio-mechanical simulations of the head and demonstrate their use for solving advanced problems in a clinical environment.

---

[*]   Max-Planck-Institute of Cognitive Neuroscience, Stephanstrasse 1, D-04103 Leipzig, Germany

2. BIOMECHANICAL FORWARD MODELS

With so-called forward models, direction and magnitude of forces acting onto an object are known. The deformation due to these forces is sought for. As an example, we studied the extent of deformation exerted by mounting a halo frame to the skull.

2.1. FROM IMAGES TO MESHES

The reliability of the complete FE analysis package depends on the precise delineation of objects of interest and their associated properties derived from multimodal imaging data. The imaging data of the individual body part of interest (BOI) first has to be segmented into the different anatomically defined tissues, i.e. materials have to be detected and defined in the raw dataset. Based on the segmented image datasets and on the individually measured and calculated material properties high quality finite element meshes have to be created to warrant the accuracy of the simulation results and to describe the BOI as precise as possible.

In order to setup biomechanical forward models of the human head, the compartments skull, white and grey matter of the brain, cerebro-spinal fluid (CSF), and extracranial tissue are segmented. To define these compartments, T1- and PD-weighted 3D datasets must be acquired. The first processing step consists in converting all data into a common proprietary format called Vista [5]. Then, the T1-weighted dataset is registered with the PD-weighted dataset, interpolating both to an isotropical voxel dimension of 1 mm. Next, both aligned datasets are segmented while correcting for intensity inhomogeneities of the B1 scanner field into 3 classes (T1) resp. 2 classes (PD). On output, a set of probability volumes (one per class) is produced, which is analysed further. The skull and extracranial tissue compartment are segmented from class 1 of the PD-weighted dataset by simple thresholding and morphological post-processing. The intracranial portion is masked using the skull mask. The T1-weighted dataset is used to define the white matter and grey matter compartments, which are found from the intracranial portions of class 2 (resp. 1) The remaining intracranial voxels are addressed as CSF. All compartments (skull, extracranial tissue, white matter, grey matter and CSF) are composed in a single volume dataset and labelled to be compliant with the material database (see Fig. 1). CT datasets of the head are much easier to segment, as we are interested in discriminating soft tissue from bone only. However, the gantry and head holders should be removed for modelling, so some preprocessing is required.

Once a suitable segmentation is achieved, the next step is to introduce a FE mesh in the segmented BOI. The basic idea of our mesh generation algorithm is to exploit the predefined spatial discretisation inherent in a medical scan dataset. The algorithm evolves in three steps:

(1) The input image is first decomposed into hexahedral elements. Their edge length e_{min} is user-defined in terms of voxel edge lengths. A material label is assigned to an element according to the segmentation result. (2) The isotropic subdivision is followed by a collection step. By recursively traversing the isotropic hexahedral mesh, elements of identical material labels are collected to form cells with larger edge lengths. A cell inherits the material label of its building bricks. The maximal edge length e_{max} is another user-defined parameter. (3) Because many of the cells now have nodes on their edges and faces, a subdivision of cells into tetrahedra is generated. If a cell contains eight nodes, the cell is regularly subdivided into 6 tetrahedra. Cells containing more than eight nodes are tesselated by a Delaunay algorithm [3]. Since rarely more than 20 nodes are

encountered, the tesselation is stable and fast. A tetrahedron inherits its material label from its mother cell.

Advantages of this algorithm are: (1) It is fast. Producing a mesh of about 200000 elements takes 30 s on a PC. (2) Just two parameters (e_{min}, e_{max}) influence the number of elements to be created. (3) Tetrahedra produced have guaranteed geometrical properties. (4) Node numbering is suitable for setting up sparse linear equation systems.

Information about mechanical tissue properties were collected by an extensive literature review and by ex-vivo experiments using animal tissue. The material database is available to the public [1]. Material parameters are addressed to the elements of the FE mesh, corresponding to their material label (see Fig. 2).

2.2. FINITE ELEMENT MODEL ANALYSIS

The numerical solution system (NSS) plays an important role within this generic environment. Input for the solution system are FE meshes generated by the software described in the previous chapter. The NSS allows efficient, generic load balancing and equation solving on parallel HPC systems. For biomechanical simulations of the human head, the HeadFEM application is provided.

HeadFEM was designed as an object oriented modular code using the Finite Element Interface (FEI) as defined by Sandia National Labs [4] to allow a clean integration of solver libraries and to facilitate further enhancements of the software. The DRAMA library [2] is used for dynamic load balancing. Although the library was originally developed for applications with dynamic, solution-adaptive mechanisms, it can equally well be applied to static problems. Based on a very general cost model, DRAMA provides access to a range of parallel partitioning algorithms through a simple and effective mesh-based interface. The repartitioner tool based on the DRAMA library provides load-balancing, matrix partitioning and basic data-migration capabilities to the NSS components. It supports different material models in the form of material labels for the elements. Linear elastic and non-linear hyper-elastic FE analyses of tetrahedral and hexahedral meshes are supported in HeadFEM. The non-linear analysis is implemented by a full Newton-Raphson method based on a calculation of the tangential stiffness matrix. A mixed displacement/pressure formulation implemented by the mean dilatation method allows modelling compressible and nearly incompressible materials like soft tissue. Suitable non-linear stress/strain measures have been implemented in the code. The FEI matrix interface links HeadFEM to the parallel linear solver library PILUTS (Parallel Incomplete LU with Threshold preconditioned Solvers). This library includes parallel sparse solvers for real symmetric positive definite (spd), general real symmetric and real non-symmetric matrices. The results of a linear or non-linear static FE analysis with HeadFEM are vectors of nodal displacements and forces and element based stresses and strains. A typical calculation time for a static linear / non-linear FE analysis is less than 5 / 30 minutes for a problem with 200000 elements corresponding to a spatial resolution of 2 mm on 8 CPUs.

2.3. FORWARD MODELS IN FACIAL SURGERY

The Clinic for Maxillo-Facial Surgery at the University Clinic of Leipzig is treating patients with in-born deformations of the skull. A stereotactic frame (a so-called *halo*, see Fig. 3) is mounted to the head by three fixation screws on each side of the head. During surgery, sub-parts of the skull are mobilised and attached to the frame by wires. Pulling wires in a certain direction at a certain distance per day will bring skull parts slowly to a desired position, thus correcting the skull deformation. Typically, 1mm shifts per day are achieved, and after 4-5 weeks, are clinically sufficient results is obtained. Because skull parts are now in their "natural" position (and under natural load conditions), a self-contained healing process is induced. The choice of the direction and speed applied to the wires attached to the skull parts is currently driven by clinical experience only. The outcome of the procedure may be optimised by simulations in terms of restoration precision and treatment time. From a group of 22 patients with in-born deformations of the skull, spiral CT images were be obtained in a native state (TP1), after halo fixation (TP2), before halo unmounting (TP3) and at treatment end (TP4). An example patient case is shown above (see Fig. 3), the result of the forward model below (see Fig. 4).

3. BIOMECHANICAL INVERSE MODELS

With so-called inverse models, structural changes are observed by acquiring time-series images. A deformation field is derived from analysing these images, and the direction and magnitude of forces acting onto these structures are sought for. As an example, we demonstrate the analysis of the brain shift phenomenon during neurosurgical interventions.

3.1. PROCESS CHAIN FOR INVERSE MODELLING

Structural changes due to brain growth, ageing, surgical intervention or pathological processes may be detected by registration of time-series Magnetic Resonance Imaging (MRI) data. Our approach consists of six steps: (1) alignment of individual scans with the stereotactic co-ordinate system, (2) correction of intensity inhomogeneities of the scan data, (3) linear registration of the follow-up scans with the initial one, (4) intensity adjustment between all scans, (5) non-linear registration of all scans for yielding a deformation field, (6) analysis of the deformation for critical points. Step (1) is carried out to allow inter-subject comparisons, step (3) is included to correct for differences in position and orientation; image intensity histograms have to be adjusted (step (4)) as the following non-linear registration step uses an intensity-based cost function.

The critical step of this processing chain is non-linear registration. In order to yield a biophysically plausible result, a physics-based model is needed. Because large deformations (i.e., greater than 10 mm) are found when modelling the brain shift, a viscous-fluid approach (see Fig. 5) is most promising. When a careful optimisation for solving the underlying PDE is applied [8], single processor computation times of about 15 min on recent PCs are achievable.

The resulting deformation fields are large and, thus, hard to interpret (see Fig. 5). Clinical applications call for an intuitive visualisation of complex phenomena. For a simplified but sufficient description of these deformation fields, contraction mapping is applied to detect critical points (step

6) that reflect the topology of the vector field [7]. Finally, visualisation includes the calculation of surface meshes, mapping of vector field data, coding of trajectories and critical points. An example result is shown in Fig. 6. Repellors (green spots) denote areas where an atrophy in adjacent cortical areas was found. The little arrows correspond to a virtual "flow of mass" from frontal to parietal brain compartments. Areas shaded in blue move inward with time, those in red outward.

As a clinical example application, we studied the brain shift phenomenon during neurosurgical intervention. MRI scans were acquired by an Open MR scanner before opening the skull and at certain timepoints during the intervention (see Fig. 7).

Obtained deformation fields demonstrate that the brain shift mostly follows gravitational forces. However with frontal osteotomy, the shift is confined to the ipsilateral hemisphere, as the falx cerebri in the interhemispheric cleft mechanically decouples both hemispheres to a certain extent. The largest deformations are found at the border of the lesion (up to 30 mm in this case). The computed deformation fields may be used to adapt pre-operatively acquired functional images (fMRI or PET) to the actual status, thereby guiding the surgeon to preserve eloquent brain structures during the intervention.

BIBLIOGRAPHY

[1] AIMEDIEU P., GREBE R., The VivMat-Site. http://www.u-picardie.fr/labo/UGBM/, 2003.
[2] BASERMANN A., FINGBERG J., LONSDALE G., MAERTEN B., Dynamic multi-partitioning for parallel finite element applications. Proc. Int. Conf. ParCo'99, pp. 259-266, Imperial College Press, London, 2000.
[3] CLARKSON K.L., MEHLHORN K., SEIDEL R., Four results on randomized incremental constructions. Computational Geometry: Theory and Applications 3, pp. 185-212, 1993.
[4] CLAY R.L., MISH K.D., OTERO I.J., TAYLOR L.M., WILLIAMS A.B., An annotated reference guide to the finite element interface specification. Sandia Report SAND99-8229, http://z.ca.sandia.gov/fei/, 1999.
[5] POPE A.R., LOWE D.G., Vista: A software environment for computer vision research. Computer Vision and Pattern Recognition (CVPR'94), pp. 768-772. IEEE Press, Los Alamitos, 1994.
[6] The SimBio Project, http://www.simbio.de, 2003.
[7] TITTGEMEYER M., WOLLNY G., KRUGGEL F., Visualising deformation fields computed by non-linear image registration. Computing and Visualization in Science, Vol. 5, pp. 45-51, 2002.
[8] WOLLNY G., KRUGGEL F.; Computational cost of non-rigid registration algorithms based on fluid dynamics. IEEE Transactions on Medical Imaging, Vol. 21, pp. 946-952, 2002.
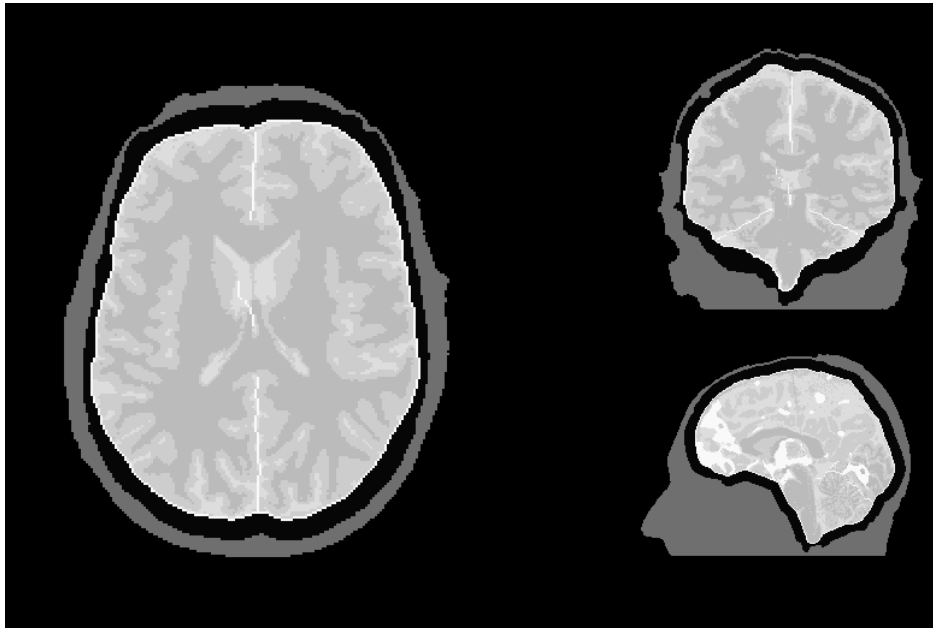
Fig.1: Segmentation of an example MRI dataset: Skull (black), extracranial tissue (dark grey), white matter (grey), grey matter (light grey), CSF(white)
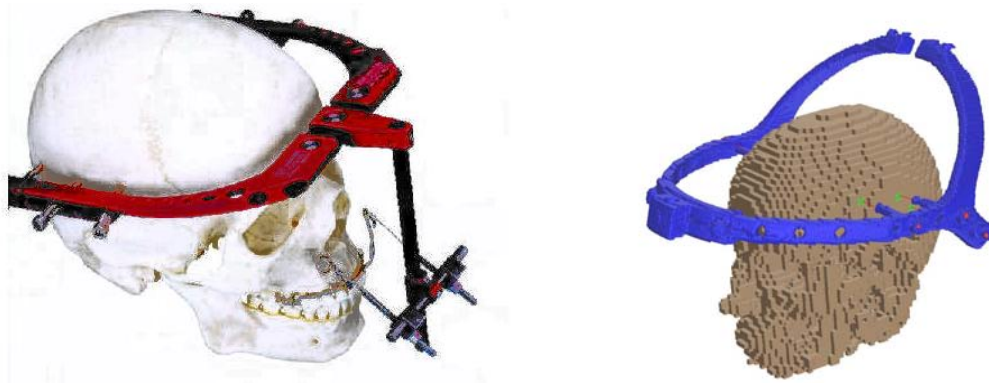

Fig.2: (Left) A halo frame (the u-shaped device) and a distractor (the vertical bar) is mounted to a skull. (Right) FE mesh at a resolution of 2 mm generated from medical scan data.
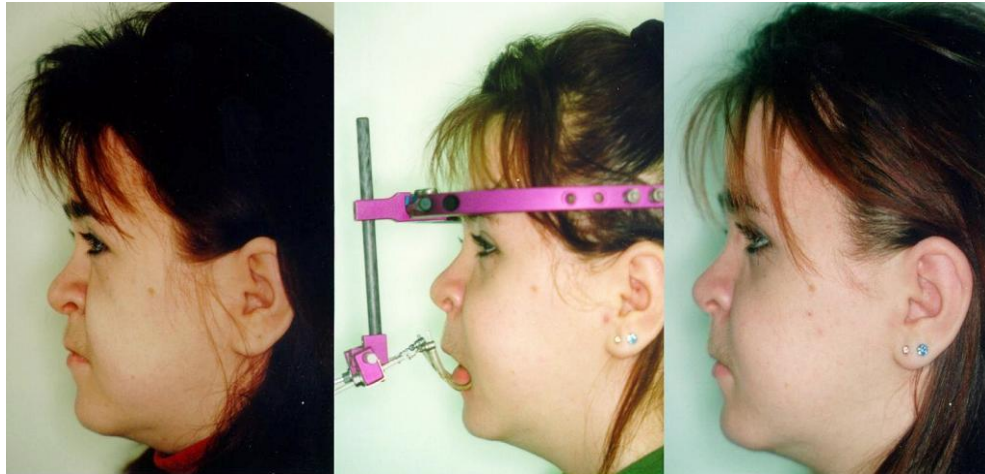
Fig.3: (Left) Lateral view of a patient suffering from a dysplasia in the midface. (Middle) After mounting the halo frame and distractor. (Right) Result of distraction osteogenesis.
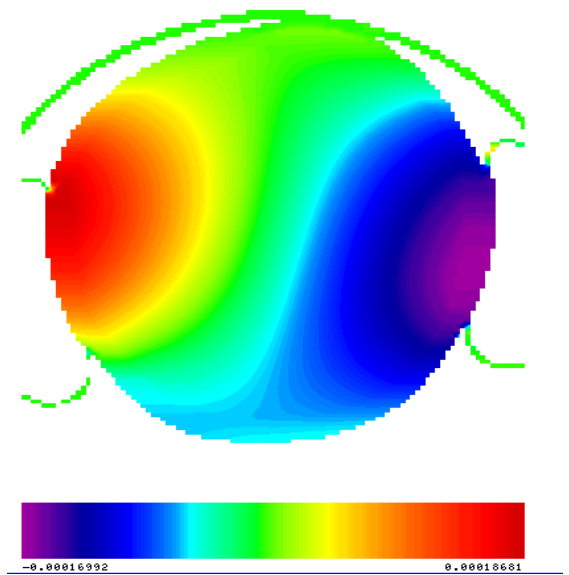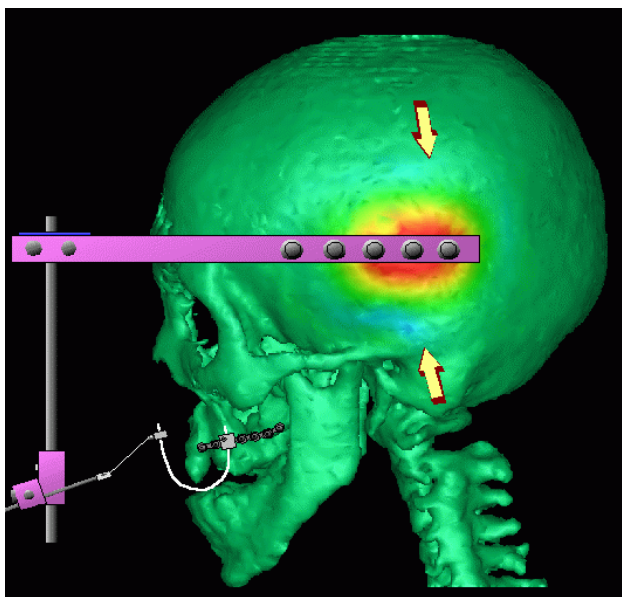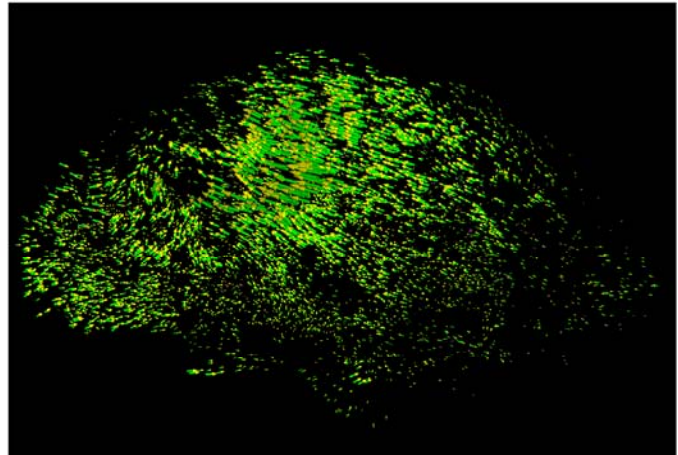

Fig.4: (Left) The halo frame exerts a force onto the skull. Red areas denote an inward deformation, while blue areas (see arrows) correspond to an outward deformation. (Right) A stress plot of a head slice at the halo position.

Fluid Dynamic Image Registration
(registration result)

$$\hat{h} = \arg\min_{h} \int (S(x) - R(x))^2 \, dx + \kappa L v$$

where L is confined to visco-elasticity, via

$$L = \mu \nabla^2 + (\lambda + \mu) \nabla \nabla \cdot$$

and the connection between v and h at time t is given by

$$v(x,t) = \frac{\partial h(x,t)}{\partial t} + \nabla h(x,t) v(x,t).$$

Result: displacement (vector) field

Fig.5: Non-linear registration of time series data is the critical step of inverse biomechanical simulation. Here, a model based on visco-elasticity is used that is able to model large deformations
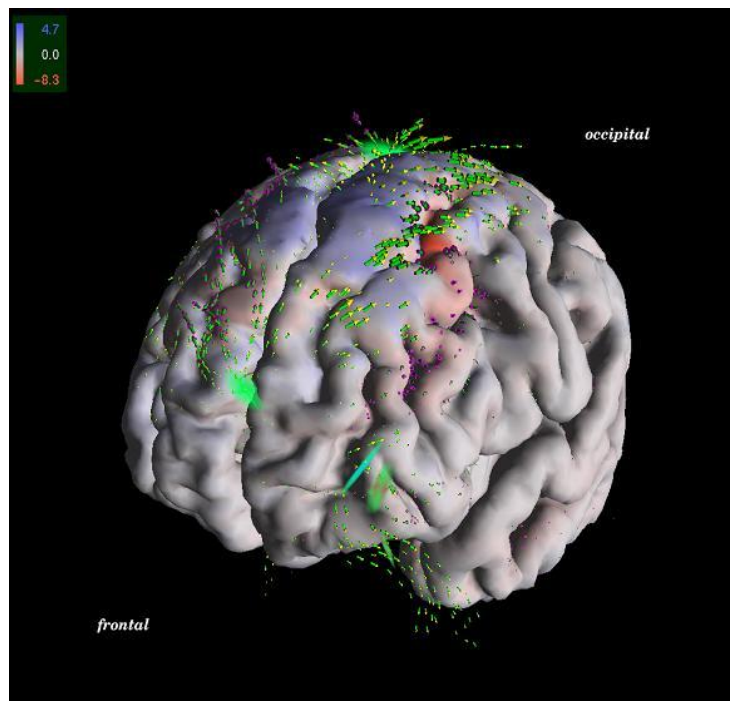

Fig.6: Example visualisation result of an inverse biomechanical model. Repellors (green spots) denote areas where an atrophy in adjacent cortical areas was found. The little arrows correspond to a virtual "flow of mass" from frontal to parietal brain compartments. Areas shaded in blue move inward with time, those in red outward
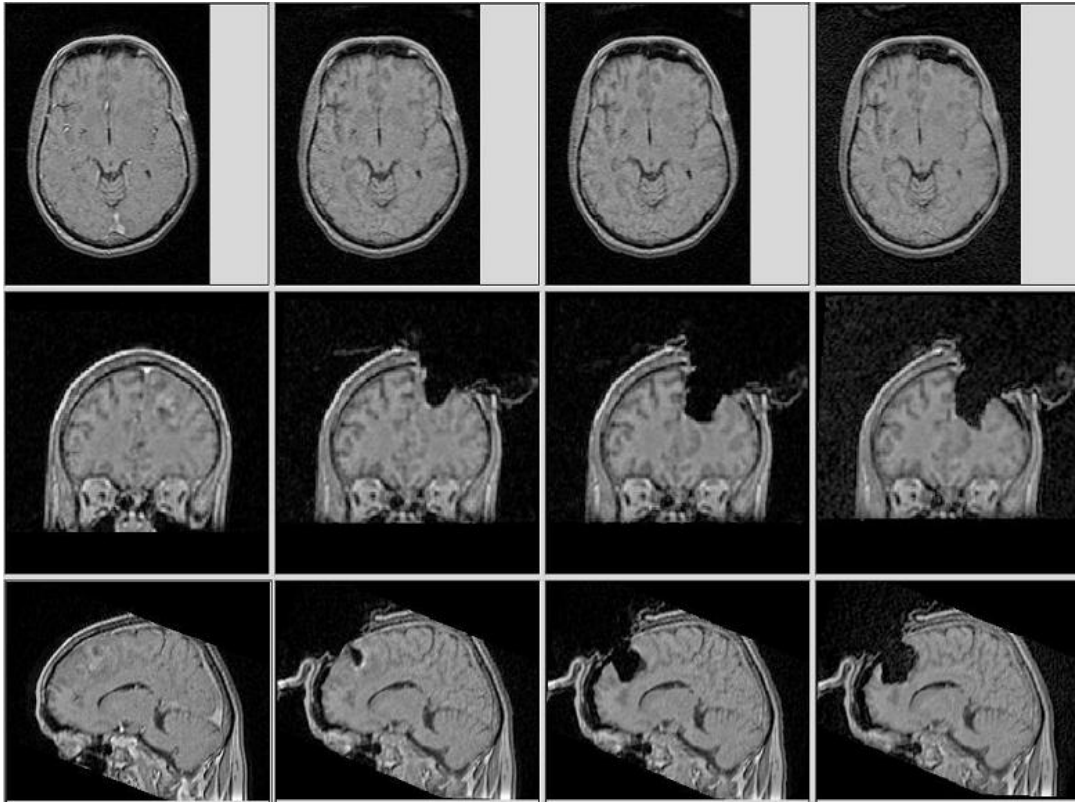
Fig.7: Intra-operative MRI scans acquired before opening the skull (left) and at certain timepoints during the intervention. The brain deformation is best observed on the sagittal scans (bottom row).
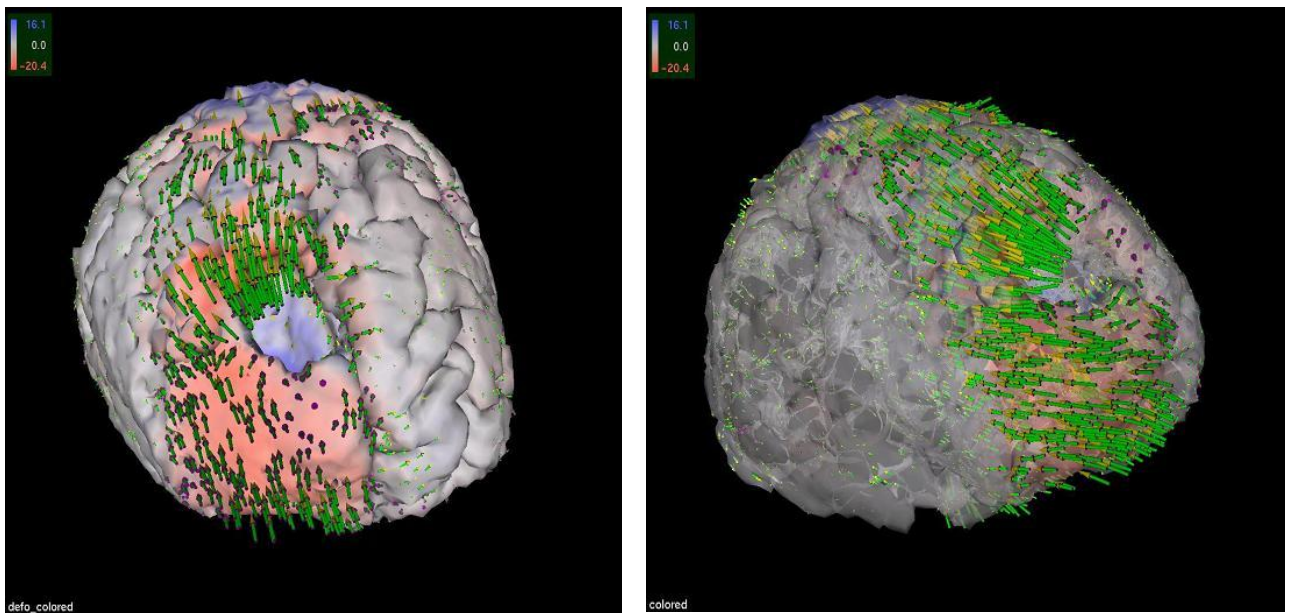

Fig.8: Frontal (left) and temporal (right) view of the deformation field due to the brain shift phenomenon. The shift follows gravity in a fronto-occipital direction, but is mostly confined to the right hemisphere.